Through-the-Body Localization of Implanted Biochip in Wearable Nano-Biosensing Networks

Haochen Hu, Zhi Sun, and Josep M Jornet
Department of Electrical Engineering, University at Buffalo, State University of New York, Buffalo, NY 14260
E-mail: {haochenh, zhisun, jmjornet}@buffalo.edu.

***Abstract*—Recent developments of nanotechnology are enabling new smart health monitoring and diagnosis systems based on wearable nano-biosensing networks. Such systems consist of at least one biochip implanted inside the human body and a wearable device that can activate nanosensors on the biochip and take measurements. Due to the motion of the human body, the wearable device may become misaligned with the implanted biochip. Since passive nanosensors and weak signals are utilized to protect biological tissues, such misalignment can significantly impact the sensing accuracy and even feasibility. Therefore, the relative position between wearable device and the implant has to be determined so that the wearable device can compensate the impacts of misalignment. There are two critical problems of through-the-body localization: 1) reflections from the biochip behind biological tissues are shadowed by reflections from tissues, which tend to dominate a long duration of time, and 2) the position of the implanted biochip cannot be calculated with a specific model of biological tissues. In this paper, a through-the-body (TTB) localization mechanism is proposed to estimate the position of implanted biochip without a priori knowledge of biological tissues of human body. The localization mechanism utilizes spatial filtering to mitigate reflections from biological tissues and uses support vector machine (SVM) regression to estimate the position of the implanted biochip. Through the analytical modeling and numerical simulations, it is shown that the reflections from biological tissues can be effectively mitigated by spatial filtering and SVM regression can estimate the position of the implant with high accuracy.**

I. INTRODUCTION

In recent years, the development of miniature nanosensors that can measure biological interactions at the nanoscale has enabled health monitoring and diagnosis systems based on nano-biosensing networks. The nano-biosensing networks can operate inside human body to detect biological interactions. The nano-biosensing networks can also be utilized for monitoring the vital signs of soldiers such as detecting if the wearer is immobile or unconscious in the battlefield in the future. As shown in Fig. 1, the system of biosensing networks contains at least one implanted biochip and a wearable device that is able to collect signals of nanosensors. The biochip is implanted in the wrist, embedded in human tissues such as skin, blood, and fat. On the one hand, there is an array of passive nanosensors that are based on surface plasmon resonance (SPR) placed on the implanted biochip to detect biomarkers that are defined by immobilized selected chemicals of diseases flowing in the body fluids, such as different types of cancer [1-2]. On the other hand, the wearable device consists of an array of co-located optical nano-sources and nano-detectors for distributed excitation and signal collection, respectively. To prevent biological tissues from being damaged by high temperature that results from molecular absorption [3], the signal transmitted by the optical sources is purposely

This work was supported by the National Science Foundation under Award IIP-1718177.

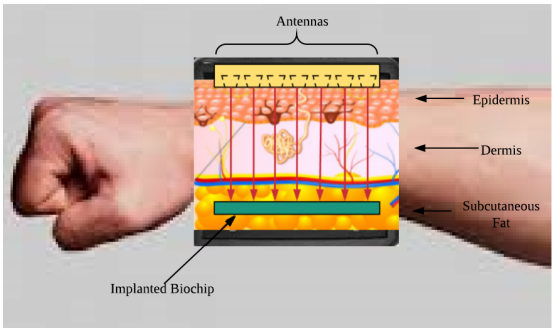

Fig. 1: Health monitoring and diagnosis system based on nano-biosensing networks

low, which leads to low signal to noise ratio (SNR). Ideally, if there is a perfect alignment between the biochip and the wearable device, all the nanosensors can be activated and their reflections can be captured by detectors on the wearable device. However, due to the motion of human body, any misalignment between the wearable device and the biochip can seriously reduce the sensing accuracy. Although beamforming with optical nano-antenna arrays can be utilized [4] on the wearable device to mitigate effects of misalignment and obtain reliable sensing results, spatial information about the position of the implanted biochip is needed to set up parameters of beamforming in advance. Thus, it is very important to know the position of the implanted biochip for nano-biosensing networks.

Localization of the implanted biochip encounters two major challenges. First, the reflections from biochip are shadowed by strong reflections from biological tissues. When nano-antennas on the wearable device collect signals to localize the implant, only reflections from the implanted biochip contain useful spatial information that can be used for the localization. Due to the absorption phenomena, when the signals propagate through the biological tissues, the signals that reach the implant and then return to the wearable device are highly attenuated. On the contrary, reflections from biological tissues that do not reach the implanted biochip are significantly stronger than reflections from the implant. Therefore, the received signals that contain all the reflections cannot be directly utilized for localization. It is very difficult to separate reflections from biological tissues and reflections from the biochip by traditional filters in time domain and frequency domain. Reflections from biological tissues are mixed with reflections from the biochip in both frequency domain and time domain, since the transmission distances of signals are short and all reflections have the same frequency. Furthermore, the mitigation strategy of reflections from biological tissues cannot depend on the channel model. The TTB localization mechanism should work with high accuracy for different people with different biological

978-1-5386-7185-6/18/$31.00 ©2018 IEEE

compositions (e.g.,skin pigmentation, fat). As for the second challenge, according to our analysis, there is not a specific model of biological tissues to calculate the position of the implanted biochip. We have to localize the implanted biochip without a priori knowledge of the human body. To our best knowledge, the research about TTB localization has not been studied before.

Existing works that deal with wall reflections are not suitable to mitigate reflections from biological tissues. Principle component analysis (PCA) based on singular value decomposition (SVD) for wall clutter mitigation in [5-7] is not suitable inside human body since the number of eigen-component that result from reflections from biological tissues are unknown. Another mitigation method that is spatial filter is proposed in [8], which considers that the wall is homogeneous and the boundaries of wall are parallel to each other. This method cannot eliminate reflections from biological tissues completely because biological tissues cannot be regarded as perfectly homogeneous and parallel layers.

In this paper, we propose a TTB localization mechanism of the implanted biochip that does not depend on the channel model and a priori knowledge of the characteristics of biological tissues. In our proposed localization mechanism, there are multiple reflectors placed on the implanted biochip asymmetrically to describe the spatial position of the implanted biochip. Optical nano-sources/nano-antennas are operated in on-off switching fashion one by one. Because of the above operations, reflections from biological tissues are mitigated by the strategy based on multilayer spatial filtering, which utilizes the strong similarity of reflections from biological tissues across different antenna positions. On the contrary, reflectors return different echoes with different antenna positions. Nevertheless, in the real life, the reflections from biological tissues cannot be perfectly removed since the the bandwidth of spatial filter is not exactly equal to the bandwidth of reflections from biological tissues in the spatial spectrum. To localize the biochip with remaining part of reflections from biological tissues after mitigation, support vector machine (SVM) is utilized in this paper to find the relationship between the position of the implanted biochip and the collected data that contains remaining part of reflections from biological tissues. For the positions and characteristics of biological tissues that are not included in training samples, SVM regression is still able to predict positions according to input features. Kernel trick is also adapted to find nonlinear relationship between positions and collected data by mapping input data onto higher dimensions. As the number of training samples becomes larger, more types of characteristics of biological tissues are contained and the effects of remaining reflections from biological tissues are further minimized.

The rest of paper is organized as following. In Sec. II, the TTB localization mechanism is presented. First, we introduce the antenna operating strategy of the localization system. Second, the multilayer spatial filter for mitigating reflections from biological tissues is analyzed. Third, explanation of SVM regression is proposed. Then, in Sec. III, we explain setup of simulation and the environment of data collection system. The test results of through-the-body localization mechanism are also evaluated in this section. Section IV concludes this paper.

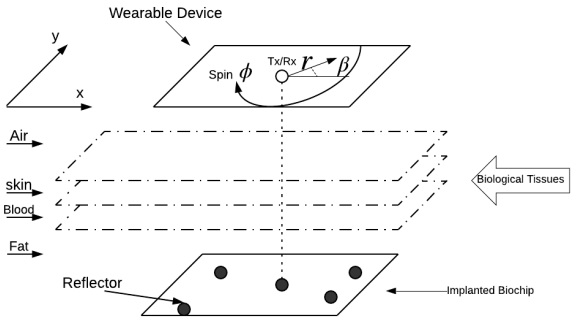

Fig. 2: Localization system of implanted biochip

II. THROUGH THE BODY LOCALIZATION MECHANISM

In this section, we first propose the TTB localization system and antenna operation framework that is utilized to detect the implanted biochip. Then, the mitigation method of reflections from biological tissues is analyzed. At the end of this section, SVM regression is introduced for estimating the position of implanted biochip.

A. TTB Localization System and Operation Framework

Different from the common localization techniques that only estimate the position of target as an integrated entity, we propose the TTB localization system that is able to estimate finer position of each nanosensor on the implanted biochip. As we mentioned in section I, there are multiple nanosensors on the biochip, and the wearable device needs to know the position of each nanosensor to set up parameters for beamforming. As shown in Fig. 2, multiple reflectors are placed on the implanted biochip asymmetrically. The relative positions between nanosensors and reflectors are fixed and known to the localization system. If positions of reflectors are figured out, the positions of nanosensors can be calculated as a result.

Thus, we define 3 parameters r, β, and ϕ, to describe the positions of the reflectors. r is the horizontal distance between the center of wearable device and the reflector on the center of the implanted biochip. β is the angle between direction of r and x-axis. Since in the real life, wearable device has slightly self spin due to the motion of human body, we also define parameter ϕ to describe such spin. Those three parameters are estimated by SVM regression with the received signals processed by spatial filter. In addition, the depth of the implanted biochip is not considered in localization mechanism since the information of relative position between the wearable device and the implanted biochip is enough to set up parameters for beamforming technology.

For the mitigation of reflections from biological tissues, we propose a particular antenna operation strategy. Antennas are arranged into a matrix with a rows and b columns. Distances between two adjacent antennas in a row are the same. In addition, optical antennas on the wearable device are highly directional, which means that the illumination area on the biochip of each antenna is limited. It is worth noting that all antennas do not work at the same time. At a single time slot, only one antenna element is working for signal transmission and reception. Antenna element is turned on and off one by one in a row, and then we repeat the same operations in the next row of antennas. In the localization system, the wearable

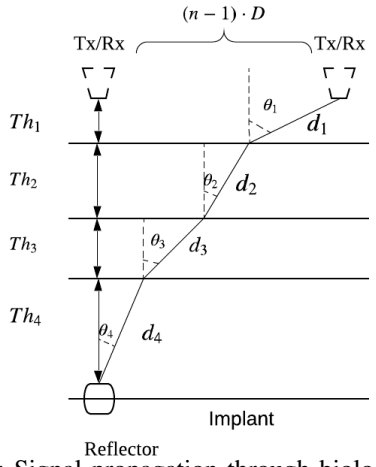

Fig. 3: Signal propagation through biological tissues

device is deployed to be parallel to the surface of skin so that antenna array is parallel to the skin. The implanted biochip is also deployed to be parallel to the skin. For the discrete signal, the collected data can be arranged into B-Scan matrix:

$$B = (C_1, C_2, ..., C_N), \tag{1}$$

where column $C_n = (c_{n1}, c_{n2}, ..., c_{nM})^T$ means the data collected at n_{th} antenna position in M sampled time. M and N represent the total sampled times and overall antenna observation positions respectively. Each row of B-Scan matrix contains the data received at the same time point in N positions.

B. Removal of Biological Tissues Reflection

We start from considering an ideal model of biological tissues where medium of each layer is assumed to be homogeneous and boundaries of layers are parallel to each other. Next the analysis of signal in practical model is provided. When n_{th} antenna is working for detection, the total received echoes consist of four contributions:

$$E(n,t) = E_s(t-\tau_s) + E_b(t-\tau_b) + E_f(t-\tau_f) + E_n(t-\tau_n), \tag{2}$$

where $E_s(\cdot)$, $E_b(\cdot)$, and $E_f(\cdot)$ are the the biological tissues reflections from skin, blood and fat. τ_s, τ_b and τ_f are their corresponding time delay. E_n and τ_n are the reflection of reflector and time delay for n_{th} antenna, respectively. As we know the transmitting power P_t and the total attenuation L_{total}, the formulation of each reflection can be described as:

$$E(t-\tau) = L_{total} \cdot P_t \cdot e^{jw(t-\tau)}. \tag{3}$$

We define D as the horizontal distance between two adjacent antennas in one row of antenna. As shown in the Fig. 3, there is an antenna above the reflector vertically assumed as the first antenna. Distance between n_{th} antenna and first antenna is $(n-1)D$. According to the *Snell's Law*, all other refractive angles can be represented by θ_4: $sin\theta_i = \frac{n_4}{n_i} sin\theta_4$, where n_i denotes the real part of refractive index. Then total horizontal distance between n_{th} antenna and reflector can be described:

$$(n-1)D = \sum_{i=1}^{4} \frac{n_4}{n_i} sin\theta_4 d_i, \tag{4}$$

where $d_i = Th_i / cos\theta_i$ is the transmission distance in a certain medium such as air, skin, blood, and fat, as shown in Fig. 3.

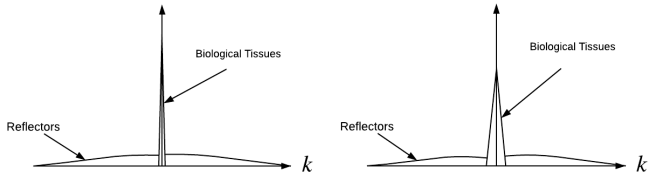

(a) In ideal model (b) In real environment

Fig. 4: Spatial frequency spectrum of received signal

Then the refractive angle θ_4 is determined by distance $(n-1)D$:

$$\theta_4 = sin^{-1}\left(\frac{(n-1)D}{\frac{n_4}{n_1}d_1 + \frac{n_4}{n_2}d_2 + \frac{n_4}{n_3}d_3 + d_4}\right). \tag{5}$$

All other refractive angles can be calculated by the same procedures. Refractive angles θ_i and transmission distances d_i change with different position of working antenna. Thus, time delay of reflector reflections for n_{th} antenna also varies with different working antenna's position since d_i is changing:

$$\tau_n = \frac{d_{skin}}{\upsilon_{skin}} + \frac{d_{air}}{\upsilon_{air}} + \frac{d_{blood}}{\upsilon_{blood}} + \frac{d_{fat}}{\upsilon_{fat}}, \tag{6}$$

where υ_{air}, υ_{blood}, υ_{fat}, and υ_{skin} are the velocities in different medium. Attenuation in dB of reflection from reflector for n_{th} antenna is:

$$L_{total} = 2\sum_{i=1}^{4}(L_{as-i} + L_{spread-i}) + \sum_{i=1}^{4}(T_{down-i} + T_{up-i}), \tag{7}$$

where L_{as-i} is the summation of scattering and absorption loss, and $L_{spread-i}$ is spreading path loss of i_{th} layer, T_{down-i} and T_{up-i} are downward and upward transmittance of i_{th} medium, respectively. Attenuations of reflections from reflector are also changing with different positions of antennas because of the changes in transmission distance d_i and refractive angles θ_i.

On the contrary, due to the fixed vertical distance of biological tissues, the time delay and attenuations of reflections from biological tissues do not change with antenna's positions since the reflections from biological tissues propagate vertically through human body, which means that transmission distance and refractive angle of biological tissues reflections keep constant. $E_s(\cdot)$, $E_b(\cdot)$, and $E_f(\cdot)$ stay constant at the fixed time. At a fixed time t_0, the received signal is:

$$E(n,t_0) = E_s(t_0-\tau_s) + E_b(t_0-\tau_b) + E_f(t_0-\tau_f) + E_n(t_0-\tau_n), \tag{8}$$

where $n = 1, ..., N$. Since the time is fixed, the received signal is now actually a function of antenna position n, and we can rewrite the above equation as:

$$E_{t_0}(n) = E^s_{t_0} + E^b_{t_0} + E^f_{t_0} + E^n_{t_0}(n), \tag{9}$$

where $E^s_{t_0}$, $E^b_{t_0}$, and $E^f_{t_0}$ are constants. Only $E^n_{t_0}(n)$ changes with the position of working antenna n. To explain, the first row of B-Scan matrix can be considered as a function of antenna position n since every element of the first row is sampled at same fixed time point. Differences among elements of first row of B-scan matrix are only influenced by the n_{th} antenna's position. The time delay τ_n and attenuation of reflections from reflector change nonlinearly with n.

For $n = 1, ..., N$, the spatial frequency transformation of

above equation is given:

$$\begin{aligned} Z(k,t_0) &= \sum_{n=1}^{N} E(n,t_0)e^{-jkn} \\ &\approx (E^s_{t_0} + E^b_{t_0} + E^f_{t_0}) \cdot \delta(k) + Z^n_{t_0}(k), \end{aligned} \tag{10}$$

where $Z^n_{t_0}(k)$ is the reflection of reflector that are distributed over spatial frequency k. However, since the reflections from biological tissues do not change with different positions of antenna, they are regarded as DC components at a fixed time. After spatial frequency transformation, reflections from biological tissues concentrate on the zero spatial frequency with a significantly highest value in spatial frequency spectrum as shown in Fig. 4(a). Then, components of reflections from biological tissues in the received signal can be eliminated by performing a proper spatial filter. In this paper, the notch filter is applied for the mitigation of biological tissues reflections:

$$H_{notch} = \frac{1 - e^{-jw}}{1 - \alpha e^{-jw}}. \tag{11}$$

However, as we mentioned, there is no perfect model for biological tissues of human body. As a matter of fact, boundaries of biological tissues can be just considered roughly parallel to each other. Moreover, each layer of tissues is not perfectly homogeneous medium. Therefore, reflections from biological tissues also change slightly with different positions of the working antenna at a fixed time point. In that case, the expression of $Z(k,t_0)$ is:

$$\begin{aligned} Z(k,t_0) &= \sum_{n=1}^{N} E(n,t_0)e^{-jkn} \\ &= \sum_{n=1}^{N} [E^s_{t_0}(n) + E^b_{t_0}(n) + E^f_{t_0}(n)]e^{-jkn} + Z^n_{t_0}(k). \end{aligned} \tag{12}$$

In the spatial frequency spectrum, the component of reflections from biological tissues still concentrates around zero spatial frequency but has slightly wider bandwidth, as shown in Fig. 4(b). The parameter α in the equation (11) can be set a smaller value to mitigate reflections from biological tissues that have a wider bandwidth in spatial spectrum, since notch filter has a wider bandwidth with a smaller α. In practical, the bandwidth of notch filter is often narrower than the bandwidth of reflections from biological tissues in the spatial spectrum. Therefore, there is still part of reflections from biological tissues remaining in the data after filtering.

C. Support Vector Machine Regression

Calculation of positions of reflectors with mitigated data faces two problems. First, the mitigated data still contains remaining part of biological tissues reflections. Second, the model of biological tissues are unknown to the localization mechanism. Those two problems lead to the fact that there is no method that can calculate positions of reflectors on the implanted biochip. To estimate the positions of reflectors with data containing part of reflections from biological tissues, SVM regression in [9] is applied, which relies on the quality of input features. Spatial filter is able to mitigate the effects of reflections from biological tissues. Thus, the changes that result from different positions of working antenna in received data also become clear to the SVM regression. The combination of spatial filter with SVM regression is able to localize the reflectors with a good performance.

SVM regression trained by a large number of samples collected from different positions of wearable device is able to find the relationship between the mitigated data and positions of reflectors. Furthermore, SVM regression is able to predict positions of reflectors when those positions are not contained in the training dataset. Considering a dataset $\{(x_1,y_1),(x_2,y_2),,,(x_n,y_n)\} \in R^N$x R, SVM regression model where the kernel trick is applied can be described as:

$$y = f(x) = \langle w, \phi(x) \rangle + b = w \cdot \phi(x) + b, \tag{13}$$

where x_n represents features that are extracted as training samples, y_n is the corresponding label, $w \in R^N$ and $b \in R$. $\phi(\cdot)$ is the nonlinear function that maps input features onto higher dimensions. $\langle \cdot, \cdot \rangle$ indicates the dot product. For SVM regression process, parameters w and b can be obtained by minimizing the following optimization problem:

$$\frac{1}{2}\|w\|^2 + C\sum_{n=1}^{N}(\zeta_i + \zeta_i^*). \tag{14}$$

subject to:

$$\begin{cases} y_n - \langle w, \phi(x_n) \rangle - b & \leq \varepsilon + \zeta_n \\ \langle w, \phi(x_n) \rangle + b - y_n & \leq \varepsilon + \zeta_n^* \\ \zeta_n, \zeta_n^* & \geq 0 \end{cases} \tag{15}$$

where ε is the allowed error on the estimation. ζ_n and ζ_n^* are the slack variables that serve as the feasible the margin for regression problem. $C > 0$ is the hyperparameter that determines the tradeoff between the smoothness of the nonlinear regression function f and the accuracy of the fitting. In this paper, gaussian kernel is utilized.

III. SIMULATIONS AND PERFORMANCE EVALUATION

In this section, the simulation setup is first discussed. Then, the efficiency of spatial filter for removing reflections from biological tissues is validated. Finally, the performance of our proposed TTB localization mechanism is evaluated.

A. Simulation Environment Setup

Our simulation is based on MATLAB and highly resembles the data collection environment inside human body. In the simulation, path loss and attenuation of optical signal are calculated to capture the effects of human body on optical signal transmission.

There are three types of path loss. First type of loss is scattering loss that can be described as: $L_{sca} = e^{\mu_{sca}d}$ where μ_{sca} is scattering coefficient and d is transmission distance. Optical signal could deviate at different angles when propagates through the particle. Second type of path loss is absorption loss that can be described as $L_{abs} = e^{\mu_{abs}d}$. Optical signal is absorbed by atoms and molecules. The third type of path loss is spreading loss. The spherical spreading of energy loss in the EM waves can be described as: $L_{spr} = 10\log_{10}(\frac{(4\pi d)^2}{D\lambda_g^2})$, where d is the transmission distance, $\lambda_g = \lambda/n_r$ is the effective wavelength in the medium and n_r is the real part of the refractive index. D is polarization coefficient. The total path loss in TTB environment can be calculated as: $L_{pathloss} = L_{abs} + L_{sca} + L_{spr}$. Reflection and refraction are also considered.

In the training phase, the received signal strengths from the center antenna and nearest 4 antennas are considered as the training features, since those received signal strengths can describe the relative position between the wearable device and

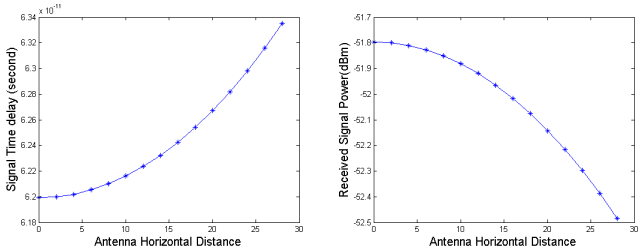

(a) Time delay versus distance (b) Power versus distance

Fig. 5: Reflections from reflector vs positions of antenna

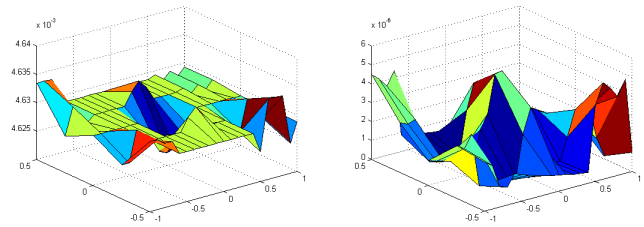

(a) Received data (b) Filtered data

Fig. 6: Mitigation of reflections from biological tissues

the implanted biochip. In addition, the summation of those signal strengths is selected as the training feature which is influenced by the distance between the implant and of the wearable device. In the SVR training process, 2 by 2 gaussian kernel is utilized. Our proposed TTB localization mechanism is designed to be able to localize the implanted biochip with different positions of wearable device.

In our simulation, there are 105 antennas distributed as a matrix with 5 rows and 21 columns. The length and width are 2cm and 1cm for both wearable device and the implanted biochip. To collect data with different positions, the wearable device moves with horizontal distance r from 0 to 3 millimeters, in the meantime, the range of moving direction β starts from 0° to 360°. Self-spin angle ϕ of wearable device ranges from $-12°$ to 12°. There are 19215 different positions of wearable device in total based on the above data collection situations.

B. Removal of Reflections from Biological Tissues Validation

We first evaluate the performance of spatial filter by examining time delay and received power of reflector reflections versus different positions of working antenna. In section II-B, we find that the reflections from biological tissues nearly stay constant at fixed time point while reflections of reflectors change with different positions of working antenna. According to our analysis, changes among reflections from reflectors are due to attenuation and time delay when signal propagates through human body. Fig. 5(b) shows received power of reflector reflection versus changing position of antenna and Fig. 5(a) shows the relationship between time delay and varying position of working antenna. In addition, x-axis represents horizontal distance in Fig. 5, which ranges from 0 to 3 millimeters. Time delay increases nonlinearly when horizontal distance r between working antenna and reflector increases, in the meanwhile, received power decreases nonlinearly due to the TTB signal model as we mentioned in section II. With that characteristics, reflections of reflectors are distributed all over the k axis in spatial spectrum after spatial frequency transformation.

The performance of mitigation method of spatial filter is evaluated by comparing the original received data with filtered data. Fig. 6 shows the value of collected data in 3-dimension from the view of wearable device. Each pixel represents the value of signal received by one antenna. In addition, Fig. 6 shows the received data in the situation where the wearable device and the implanted biochip overlaps completely in vertical. Fig. 6(a) shows the received data including biological tissues reflections and it is hard to find reflections from reflectors. Reflections from reflectors are overwhelmed by biological tissues reflection. Compared with Fig. 6(a), after spatial filtering, Fig. 6(b) provides reflections mainly from reflectors, where the peaks are the reflections from reflectors. In the meanwhile, received signal power decreases from $4.63 \cdot 10^{-3}$ nanowatts to $4.5 \cdot 10^{-5}$ nanowatts. Therefore, spatial filter can be validated as the efficient way to mitigate the reflections from biological tissues. Furthermore, with the spatial filter, the relationship between the changes of received reflections from reflectors and different positions of working antenna is more obvious for SVM regression. Trained by high quality features, SVM regression is able to estimate the positions of reflectors with a good accuracy.

C. Performance Evaluation of Through the Body Localization Mechanism

The localization tests are first performed with spatial filter, as shown in Fig. 7. The test results validate that our proposed TTB localization mechanism is able to estimate the positions of reflectors at a very high accuracy without the priori knowledge about biological tissues of human body. In Fig. 7, the y-axis represents the real labels of testing samples while the x-axis represents the predicted results of testing samples. Red line means that the real label is equal to the predicted result. We can see that most of test results concentrate around the red line with few of outliers for r, β, and ϕ.

Compared with multilayer spatial filter, second test of TTB localization mechanism is performed with the conventional SVD method without the priori knowledge of biological tissues. After SVD of collected B-scan matrix, there are three subspaces in the spectrum of singular values that are spanned by biological tissues, reflectors and noise, respectively. However, the dimension of tissues subspace is unknown because the characteristic of biological tissues varies with different human body. Without knowing the accurate dimension of tissues subspace, the removal of reflections from biological tissues has a bad performance with SVD method, which leads to the poor localization accuracy as shown in Fig. 8. Most testing samples are predicted into the values that are far away from their real labels.

In addition, to achieve more reliable results, cross validation is applied for testing the SVM regression model. Namely, testing samples are not included in the training dataset.

To further validate our proposed localization mechanism, the wearable device is placed in different positions to localize the reflectors on the implanted biochip. The x-axis and y-axis in Fig. 9 are the width and length of wearable device, respectively. We start from Fig. 9(a) with $r = 0$, $\beta = 0$ and

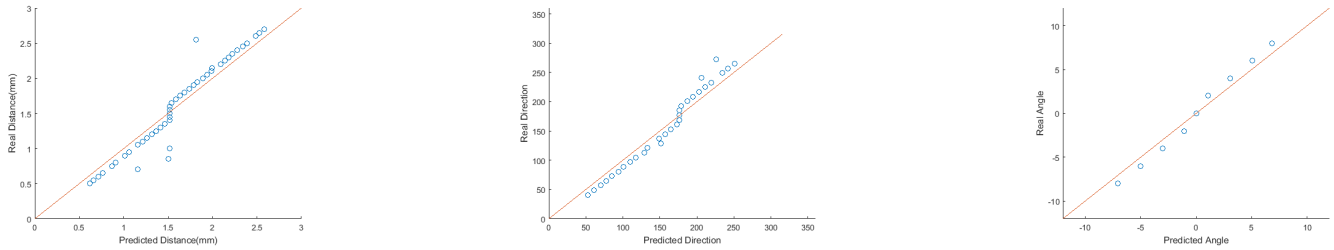

(a) Distance r test results (b) Direction β test results (c) Spin angle ϕ test results

Fig. 7: Localization performance with mitigation method of spatial filter

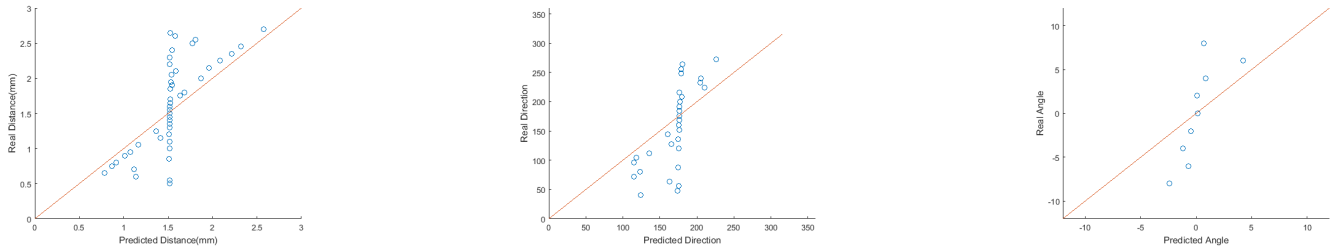

(a) Distance r test results (b) Direction β test results (c) Spin angle ϕ test results

Fig. 8: Localization performance with SVD mitigation method

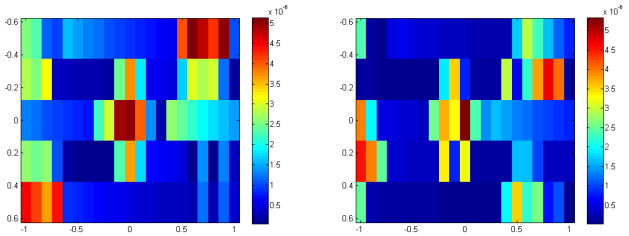

(a) r=β=ϕ=0 (b) $\beta = 7\pi/4$, $\phi = -\pi/15$

Fig. 9: Localization with different positions of wearable device

$\phi = 0$ where the wearable device and the implanted biochip are overlapping completely. From the view of the wearable device, we can identify the 5 reflectors on the implanted biochip clearly. In Fig. 9(b), the wearable device is placed in the most complicated position where the wearable device moves to the bottom right with the self spin angle $\phi = -\pi/15$. In addition, the self spin angle ϕ is considered as zero when there is no self spin. When the wearable device spins clockwise, ϕ is positive. When the wearable device spins anticlockwise, ϕ is negative. From the view of wearable device, the implanted biochip spins clockwise. The right bottom reflector is much lower than the left bottom reflector compared with Fig. 9(a).

IV. CONCLUSIONS

In this paper, we addressed the through-the-body localization problem of the implanted biochip without the priori knowledge about biological tissues of human body. Overwhelming reflections from biological tissues are mitigated by multilayer spatial filter according to the fact that reflections from reflectors are varying with different positions of the working antenna while reflections from biological tissues stay constant. Furthermore, the effects of remaining part of reflections from biological tissues on localization performance are minimized by SVM regression. SVM regression model is trained with a large amount of samples that are collected in 19215 types of position of wearable device to find the relationship between mitigated data and positions of wearable device. It shows that the proposed localization system is able to localize the implanted biochip with high accuracy. Finally, those test results mean that our proposed through-the-body localization system has a promising future in the real applications.

REFERENCES

[1] Vendrell, M., Maiti, K. K., Dhaliwal, K., and Chang, Y.-T., Surface-enhanced raman scattering in cancer detection and imaging, Trends in biotechnology 31(4), 249257 (2013).
[2] Hudson, S. D. and Chumanov, G., Bioanalytical applications of sers (surface-enhanced raman spectroscopy), Analytical and bioanalytical chemistry 394(3), 679686 (2009).
[3] H. Elayan, P. Johari, R. M. Shubair and J. M. Jornet, Photothermal Modeling and Analysis of Intra-body Terahertz Nanoscale Communication, IEEE Transactions on NanoBioscience, vol. 16, no. 8, pp. 755 763, December 2017. (2015).
[4] P. Johari, H. Pandey, A. Sangwan, J. M. Jornet, "Increasing the Communication Distance between Nano-boisensing Implants and Wearable Devices," to appear in Proc. of the 19th IEEE International Workshop on Signal Processing Advances in Wireless Communications (SPAWC), Kalamata, Greece, June 2018.
[5] Fok Hing Chi Tivive,Abdesselam Bouzerdoum,Moeness G.Amin,An SVD-based approach for mitigating wall reflections in through-the-wall radar imaging, Proc. Digit. Signal Process. Corfu (2011) 519524.
[6] M. Mohsin Riaz, A. Ghafoor, Through-wall image enhancement based on singular value decomposition, Int. J. Antennas Propag. (2012) 120.
[7] Fok Hing Chi Tivive, Moeness G. Amin, Abdesselam Bouzerdoum. Wall clutter mitigation based on eigen-analysis in through-the-wall radar imaging, Proc. Digit. Signal Process. Corfu (2011) 18.
[8] Y. S. Yoon and M. G. Amin, "Spatial Filtering for Wall-Clutter Mitigation in Through-the-Wall Radar Imaging," in IEEE Transactions on Geoscience and Remote Sensing, vol. 47, no. 9, pp. 3192-3208, Sept. 2009.
[9] A. J. Smola and B. Scholkopf, A tutorial on support vector regression, Stat. Comput. 14(3), 199222